



## **EVALUATION OF THE WEAR-RESISTANT PLATE PERFORMANCE ON DIFFERENT LOCATIONS OVER THE FLOW PATH OF A LARGE-SIZED HEAVY-DUTY CENTRIFUGAL FAN**

Nicola ALDI<sup>1</sup>, Nicola CASARI<sup>1</sup>, Michele PINELLI<sup>1</sup>, Alessio SUMAN<sup>1</sup>,  
Alessandro VULPIO<sup>1</sup>, Paolo SACCENTI<sup>2</sup>

<sup>1</sup> *University of Ferrara, Department of Engineering,  
Via Giuseppe Saragat 1, 44122 Ferrara FE, Italy*

<sup>2</sup> *Boldrocchi Group, Via Trento e Trieste, 93, 20853 Biassono MB, Italy*

### **ABSTRACT**

In industrial applications as chemical plants, cement factories, and glassmakers, large-sized centrifugal fans are commonly used for dust-laden flow processing. In many cases, the contamination is due to solid particles which are responsible for fouling and erosion issues. Erosion induces the reduction of mechanical resistance and at the same time, the modification of the geometry and the surface characteristics of the internal flow path. The process works according to the characteristics of the erodent particles, such as dimension and hardness which have to be coupled with the mechanical characteristics of the substrate, like hardness and roughness level. In addition to this, the intensity of the erosion depends on the dynamic characteristics of particles, especially velocity and impact angle. For these reasons, erosion-related issues are difficult to be predicted and reduced. In the attempt of preserving the structural integrity of the internal walls, wear-resistant plates are positioned where the impacting contaminants are supposed to be more detrimental. In the present work, a combined experimental and numerical approach is proposed to evaluate the proper set up of wear-resistance plates over the flow path of a large-sized centrifugal fan. The results show how different regions (rotating and stationary walls) are subjected to different impact behavior and for this reason, the design of the position of the wear-resistant plate is not straightforward. Suggestions related to the reduction of the erosion intensity are reported, highlighting the possibility to design the best compromise between erosion, performance, and costs.

### **INTRODUCTION**

Heavy-duty centrifugal fans are employed in process industries for cement, steel, and power production. Such machines include exhausters used for different purposes: in metallurgy, they are employed for agglomeration, where dust from the agglomeration process passes through them, or in heating and power plants where ash particles are suspended in the gas flow. Usually, these machines are tailor-made to meet the request of the customer, in terms of mass flow rate and

pressure, space constraints, structural requirements, etc. Most large centrifugal fans currently have an impeller diameter of 3 m to 4 m, with a power up to 4 MW and a running speed of 1000 rpm.

The interaction of the particles with stationary and rotating components of the machine can lead to fouling or erosion. The first phenomenon refers to the adhesion of particles to the surfaces, while the second regards the progressive removal of material from some zones of the machines. The first issue is recoverable, by cleaning the machine with on-purpose devices while the second is a non-recoverable issue, and overhaul operations are mandatory to restore the machine performance. Focusing on the erosion phenomenon, since gas velocities can reach very high values, the dragged particles possess high kinetic energy that contributes to material removal from the parts where impacts take place. The overtime blade surface worn-out pushes the fan geometry far from its design condition, leading to the reduction of the fan efficiency. Besides, the proceeding of the erosion can bring to premature failures of the most affected parts, if overhaul operations are postponed or even ignored. This is a serious threat to the reliability and the safety of the machine. The erosion damages in stationary parts are mainly related to the efficiency and reliability of the equipment, while the ones on rotating parts are also related to safety.

In 1980, the research laboratories of the Westinghouse Electric Corporation surveyed power plants having units larger than 100 MW generating capacity, and using pulverized coal-fired boilers. The results of this survey are reported in a technical report from Glasser *et al.* [1]. The findings showed that erosion damage is located mainly on blade leading-edges, trailing-edges, and fan center plates. The erosion of the leading edges was the most severe one. The Authors estimated that a total of 27,000 man-hours were being used annually to repair erosion damages in these machines and that the cost of purchasing replacement power during overhaul operation was around 11 million dollars per year.

A great number of studies in the literature is devoted to the investigation of the erosion phenomena in heavy-duty fans through numerical simulations. For the sake of brevity, only some of them are reported. Cardillo *et al.* [2] studied particle erosion in a large centrifugal fan used in cement production plants. The Authors highlighted that, in such machines, the rise of secondary flows drives the dispersion of the particles towards the blades, hub, and shroud. Castorrini *et al.* [3] investigated the effect of the erosion on an axial draft-fan employed for exhaust gas extraction in a solid-fuel power plant. The Authors detected the zones most affected by particle erosion and modified the original geometry by accounting for the material removal action of the erosion process. The erosion was found to be greater in magnitude in the suction side of the blade. The numerical erosion patterns were in qualitative agreement with the on-field observations. Aldi *et al.* [4] studied the influence of a damage in correspondence of the inlet bell-mouth of the fan. The numerical investigation showed that the presence of a damage in that zone leads to a modification of the flow field within the impeller, and to the occurrence of additional damages in zones of the fan where erosion issues were never been observed.

A common strategy to reduce the wear issue of such machines involves the use of sacrificial plates designed to resist particle erosion. Wear-resistant plates are positioned in the fan zones most affected by particle erosion. Such materials are available on the market and have different costs, depending on their performance against particle wear. The selection of wear-resistant plates and their positioning within the fan is usually driven by a mix of the manufacturer's experience and of the wear-resistant material cost.

The present work combines a numerical and experimental approach to assess the erosion intensity of the machine in order to optimize the positioning of the wear-resistant plates within the fan. First, the wear resistance of three commercial wear-resistant plates is experimentally assessed on an on-purpose developed jet-impingement test bench. Then, a fluid dynamic *simulation* has been carried out to assess the wear on the rotating and stationary parts of the machine. The machine division into patches aided to select the proper wear-resistant plate on each zone, based on the local condition of erosion severity.

## EXPERIMENTAL INVESTIGATION

The experimental campaign aims to characterize the erosion behavior of the materials at different impact angles and velocity values. The results of the erosion tests are expressed in terms of erosion rate ( $ER$ ), which is the ratio between the target mass loss after the test and the particle mass impacted on it. Generally, the erosion rate is modeled through the following relation [5]:

$$ER(V, \alpha) = K_{90} V^{n_{90}} f(\alpha) \quad (1)$$

where  $V$  is the particle impact velocity,  $\alpha$  is the particle impact angle,  $K_{90}$  and  $n_{90}$  are the erosion coefficients for the normal impingement angle, and the angle function  $f(\alpha)$  is the ratio between the erosion rate at a generic impact angle and the erosion rate at  $90^\circ$ :

$$f(\alpha) = ER_\alpha / ER_{90} \quad (2)$$

### Test bench

In the present section, the description of a jet-impingement test bench, designed and built at the Fluid Machinery Laboratory of the Department of Engineering of the University of Ferrara, is provided. The schematic view of the whole erosion facility and the main components are depicted in Fig. 1. The test bench employs dry and clean shop air provided by a screw compressor. The air is mixed with a dosed amount of powder and then accelerated in a sand-blast nozzle towards a squared specimen located in the test chamber. The nozzle outlet section has a diameter of 4 mm. An exhaust fan linked to a chimney recirculates the air inside the test chamber. The air mass flow rate is controlled by a pressure regulator upstream of the nozzle. The specimen is placed on a target holder which allows an accurate regulation of tilt angle and distance from the nozzle outlet section. For the present application, a distance of 10 mm between the nozzle and the specimen surface is chosen. Preliminary tests have been carried out employing alumina particles (with  $50 \mu\text{m}$  diameter) against C20 specimens. Through the preliminary tests, the reliability of the test bench was assessed since the results were in line with those provided by the ASTM G76 [6].

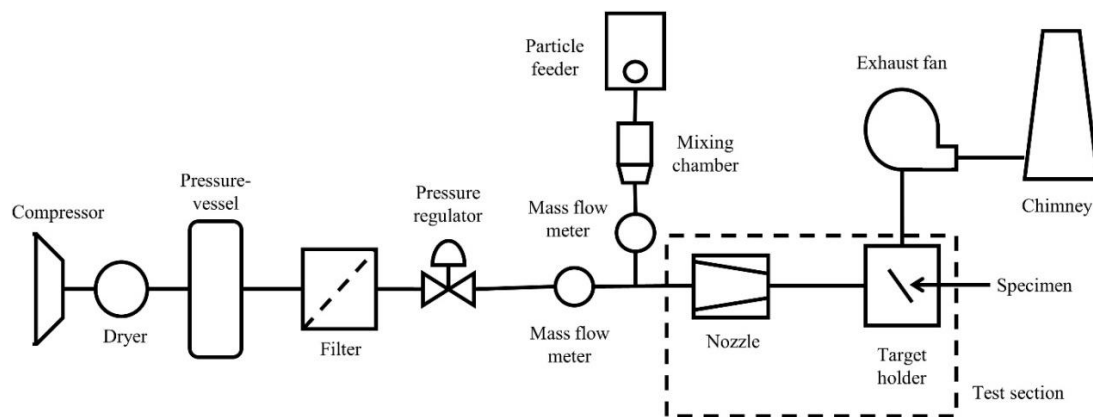


Figure 1: Schematic layout of the experimental test bench.

### Particle and substrate materials

The experimental tests have been carried out with particle and substrate materials used in heavy-duty centrifugal fan operations. The powder used in the present application is a solid material that is produced as an intermediary product in the manufacture of Portland cement. It is produced by sintering limestone and aluminosilicate materials, such as clay, during the cement kiln stage. The powder used in the present experimental campaign is collected directly from the plant where the fan operates. The powder morphology is depicted in Fig. 2a while its number and mass distribution are shown in Fig. 2b. The particle density is  $2,717 \text{ kg m}^{-3}$  and its mean diameter is  $4.34 \mu\text{m}$ . Both

particle distribution and particle density have been measured by the Malvern Mastersizer 3000 and the AccuPyc II 1340 pycnometer, respectively.

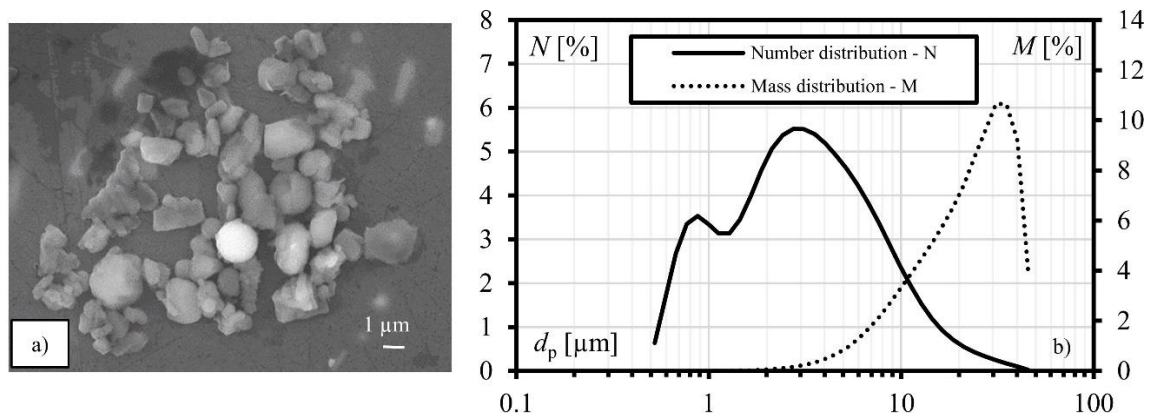


Figure 2: Characteristics of the powder employed: a) SEM observation, and b) number and mass distribution.

Three commercial wear resistant plates, named M1, M2, and M3, have been tested in the present campaign:

- M1 is a layer-composite wear plate made by the open-arc welding of a flux-cored wire DIN 8555 alloy group 10 and additional metal alloy powder. Its deposit consists of primary carbides and complex carbides in a matrix of austenite and eutectic carbides. The carbide content is 62.1 % (27.4 % primary, and 34.7 % eutectic) and has the following structures:  $\text{Cr}_7\text{C}_3$ ,  $\text{Mo}_2\text{C}$ ,  $\text{NbC}$ , and  $\text{WC}$ .
- M2 is a welding cladded layer-composite material with hard surfacing according to DIN 8555, alloy group 10, made with an open-arc welding procedure. The declared percentage of carbides is greater than 50 %. The structures of the formed carbides are  $\text{M}_7\text{C}_3$ ,  $\text{Cr}_2\text{B}$ , and  $\text{NbC}$ .
- M3 is a nickel based alloy rich of cast/crushed tungsten carbides (60 % of the coating content). The coating is composed of Ni (37 %), WC (60 %), and other components (3 %).

Due to their different chemical composition and properties, the erosion resistance of these materials changes accordingly. In particular, based on experience evaluations, the M3 showed a higher wear resistance than M2 and M1 and has consequently a higher price.

### Experimental test results and model fitting

The three materials have been tested at three mean impact velocities and five impact angles ( $15^\circ$ ,  $30^\circ$ ,  $45^\circ$ ,  $60^\circ$ ,  $90^\circ$ ). Each test has been carried out with a mass flow rate of powder of  $10 \text{ g min}^{-1}$ .

Each combination of impact angle and velocity is repeated three times on different specimens. To account for the variability related to the test procedure, an error band, calculated following the procedure reported by Schrade *et al.* [7], has been used. The experimental results are depicted in Fig. 3: Fig. 3a reports the values of the *ER* at normal impact angle, and the interpolation lines derived from Eq. 1, while Fig. 3b reports the experimental values of the angle function. The M3 plate confirms the higher resistance to particle wear. M1 and M2 have comparable wear resistance. The angle function shows a clear mixture of ductile-brittle behavior of the erosion process over the impact angle: the maximum of the *ER* is located at almost  $45^\circ$ . The three plate materials show similar trends of the angle function  $f(\alpha)$ .

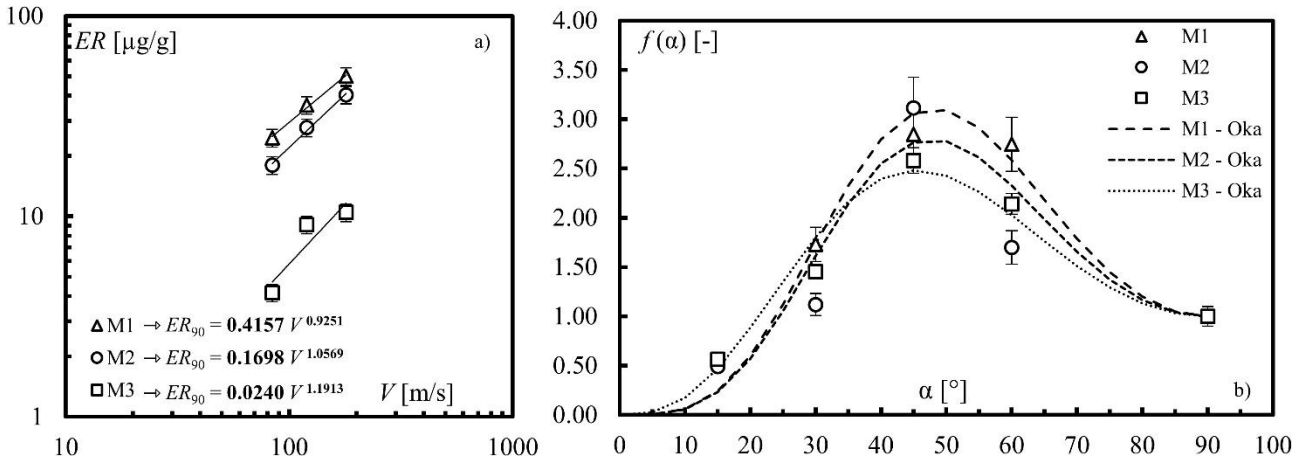


Figure 3: Results of the experimental test: a) erosion rate at normal impingement angle, b) erosion rate over the angle (experimental values and Oka's model interpolation).

To obtain a general formulation of the angle function  $f(\alpha)$ , that can be employed in numerical simulations, the experimental results have been interpolated through the Oka's model equation [8], which calculate the angle function as a combination of trigonometric functions:

$$f(\alpha) = (\sin \alpha)^{n_1} (1 + HV(1 - \sin \alpha))^{n_2} \quad (3)$$

where  $n_1$  and  $n_2$  are numerical coefficients, and  $HV$  is the material hardness expressed in GPa. The results of Oka's model interpolation are reported in Fig. 3b as dashed lines, while the coefficients employed in Eq. 3 are reported in Tab. 1 for the three tested materials.

Tab. 1: Material properties and erosion coefficients of the wear resistant plate materials.

Material	$\rho_m$ [ $\text{kg m}^{-3}$ ]	$K_{90}$	$n_{90}$	$HV$ [GPa]	$n_1$	$n_2$
M1	4,375	0.4157	0.9251	8.532	4.0	2.0
M2	7,500	0.1698	1.0569	6.767	4.0	2.2
M3	9,375	0.0240	1.1913	6.473	2.9	1.8

## NUMERICAL ANALYSIS

### Fluid dynamic simulations

The fan under examination is a large-sized single-inlet centrifugal fan, operating in a cement plant, designed and built by Boldrocchi Group. The fan is installed in the Åalborg Portland cement plant. The fan is composed of a constant-width closed impeller, with 12 backward-curved single arc blades, and a constant-width spiral volute. The rear side of the impeller disk presents 5 radial ribs for axial thrust balancing. The impeller outside diameter is 4 m and the fan design rotational speed is 652 rpm. An inlet box with 3 fixed vanes of constant thickness deflects the flow from the inlet duct, which is arranged normally to the impeller axis, into the axial direction through the fan inlet cone. The inlet cone is bolted to the front side plate of the volute, which is in common with the inlet box. Wear-resistant plates with a thickness of 10 mm are installed on the pressure side and at the leading edge of fan blades, on the inner surface of the impeller disk, on a portion of the impeller shroud near the blade trailing edge on the pressure side, and a band of the spiral volute facing the impeller outlet section. The volute and impeller of the fan are shown in Fig. 4a. To characterize the internal flow field and the particle trajectories of the centrifugal fan under investigation, a 3D fluid dynamic multiphase simulation is performed at the fan actual working point in terms of mass flow rate and total pressure rise, i.e.  $122 \text{ kg s}^{-1}$  and 8,300 Pa. The reader can refer to Aldi *et al.* [9] for all the details related to the CFD simulation setup and validation.

### Strategy of fan surface patching

To quantify the wear severity on specific zones, the machine is divided into patches, according to the scheme reported in Fig. 4.

The impeller has been divided into three zones: hub, shroud, and blades. Hub and shroud are divided according to a radial discretization. The hub (Fig. 4b) is divided into five circular areas, named progressively from R1 to R5, with thicknesses of 355 mm, 385 mm, 440 mm, 435 mm, and 435 mm, respectively. The shroud (Fig. 4c) is divided into three circular areas, named R3, R4, and R5. The sizes of R3, R4, and R5 are the same as the corresponding areas on the hub. The shroud patching accounts also for the additional wear protection plate (named TE) positioned on the trailing edge zone of the blade, in correspondence with the blade pressure side. Both hub and shroud have no axial division. Each blade has been divided into seventeen patches: one patch for the leading edge, eight patches on the pressure side, and eight patches on the suction sides (Fig. 4d). Both the pressure side and suction side of each blade have been divided into two axial zones (A1, and A2), and three radial zones (R3, R4, and R5). The radial division has been done following the R3, R4, and R5 divisions previously described on hub and shroud.

The volute has been divided into three main zones: the front side, the lateral side, and the backside. The volute front and back sides have been divided into two radial sectors named R1 and R2 (Figs. 4e and 4f). The circular area named R1 is placed at the center of the volute and has a diameter of 4.40 m, which is similar to the impeller diameter. The R2 sector comprises the remaining part of the volute front and back cases. The lateral side has been divided into three axial sections (A1, A2, and A3) each of them with a thickness of 510 mm (Fig. 4g). The volute cut-off is of great interest for particle wear, since it is a zone that can be strongly affected by erosive processes. For this reason, the cut-off zone has been isolated and analyzed separately.

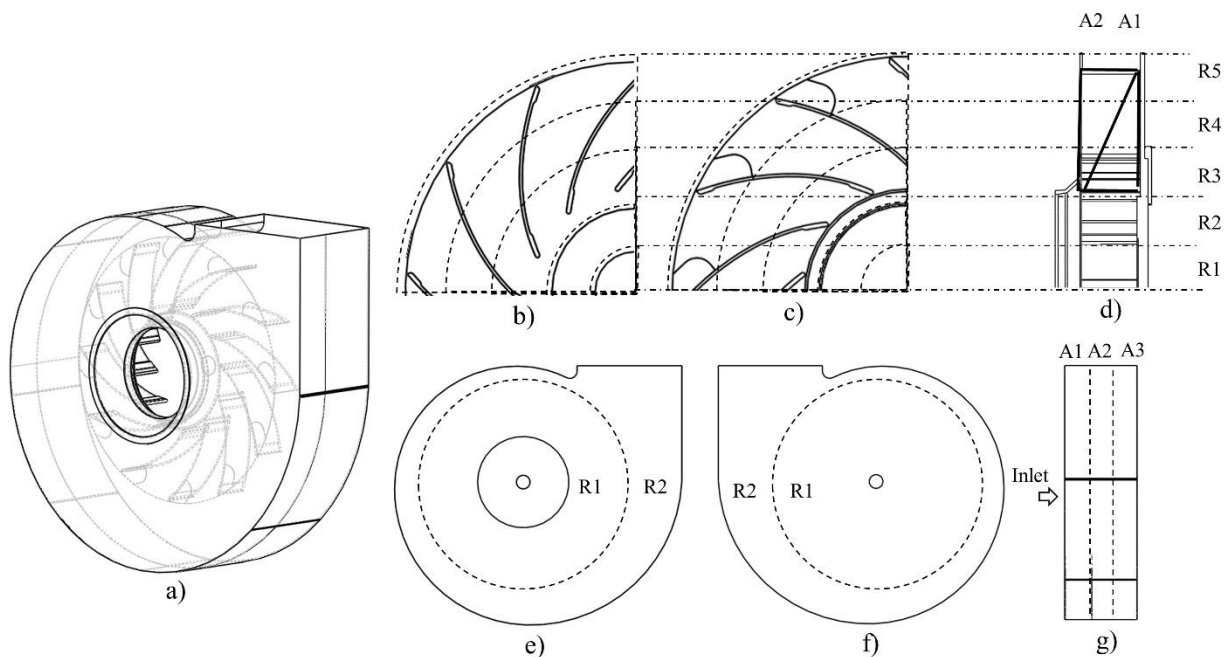


Figure 4: Strategy of fan surface patching: a) fan model, b) hub, c) shroud, d) rotor, e) volute front side, f) volute backside, and g) volute lateral side.

## RESULTS

The complex flow field developed within the fan, and the high separation zone which arises, require the use of numerical simulation to predict the impact patterns on the fan components. The CFD simulation allowed to track the particle trajectories and obtain information related to the impacts of the particles on the fan surfaces. For the present analysis, it is supposed that all the fan internal

surfaces are covered with wear-resistant plates. The wear on the fan zones is calculated by implementing Eq. 1 and 3, based on the results of the CFD simulation, and using the coefficients in Tab. 1 for the three wear-resistant materials. The results are reported in terms of average thickness reduction ( $\Delta l$ ) over 8,000 hours (almost one year) of operation on each patch of the fan.

### Hub and shroud

Figure 5 reports the thickness reduction on the shroud (Fig. 5b) and the hub (Fig. 5c). According to the experimental results, M1 shows the worst performance in terms of wear resistance. Looking at the shroud, the three materials have different trends over the radial direction. This is mainly due to the different angle functions measured during the experimental tests (Fig. 3b). This effect is visible by comparing M3 and M1 over R3, R4, and R5. However, the higher wear intensity is found in the zone near the trailing edge, named TE. For all the materials, the wear on the hub is high in the R1 zone and decreases over the radial direction until R3, and slightly increases again towards R5. The center of the disc (R1) is critical since its positioning in front of the inlet section promotes a high impact frequency in that zone.

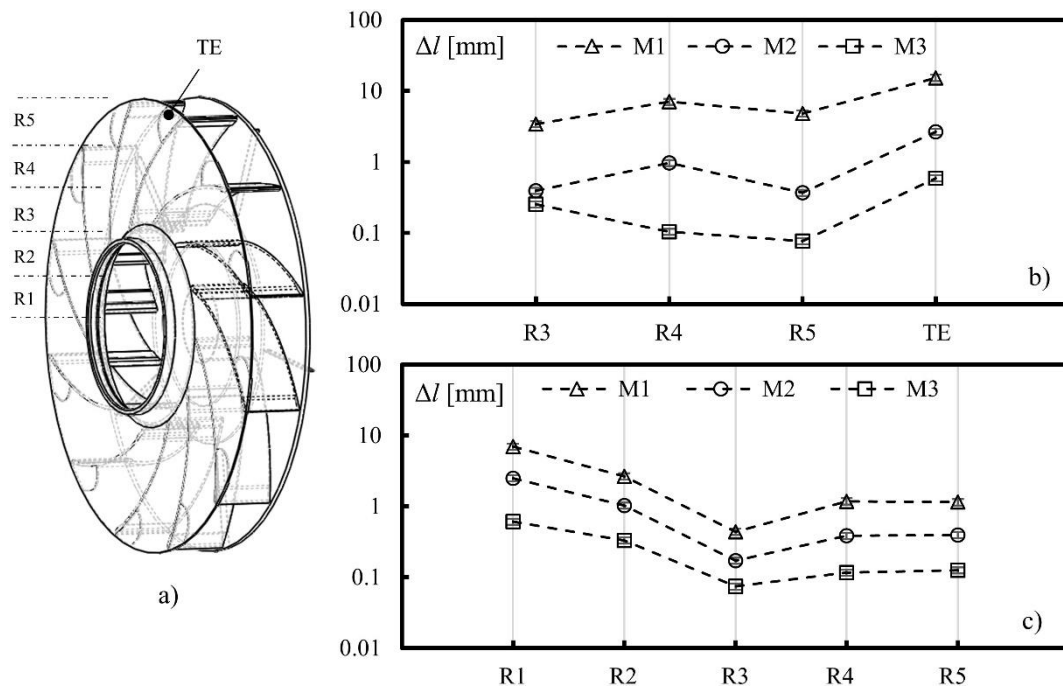


Figure 5: Rotor wear: a) coordinates of the patches and material loss b) on the shroud and c) on the hub.

### Blades

Figure 6 reports the results for the blade pressure side (Figs. 6b and 6c) and suction side (Figs. 6e and 6f). The leading edge results are included in Fig. 6b. Regarding the pressure side of the blade, the wear severity decreases over the radial direction for the portion of the blade near the hub (A1) and increases over the radial direction for the portion near the shroud (A2). However, the wear on the A1 zone is more severe than A2. In particular, the leading edge is the impeller zone that experiences high material loss. The trends of  $\Delta l$  for the three materials, over the radial direction, are similar but shifted on the y-axis, highlighting the different wear resistance of the three plate materials. Regarding the suction side of the blade, the wear is almost uniform on the whole surface for a fixed plate material.

### Volute

The results of the volute wear are reported in Fig. 7 for the front side (Fig. 7b), backside (Fig. 7c), lateral side (Fig. 7d), and cut-off (Fig. 7e). The wear severity on the stationary parts is lower than

the rotating part. This is mainly due to the lower particle impact number and impact velocity on these zones. The front side, back side, and later side have similar values of thickness reduction after 8,000 hours of operation. The cut-off is the most critical part of the volute: the wear severity increases over the axial direction. The maximum thickness reduction is found in the axial sector in front of the impeller outlet section, reaching a thickness reduction of 3 mm after 8,000 of operation.

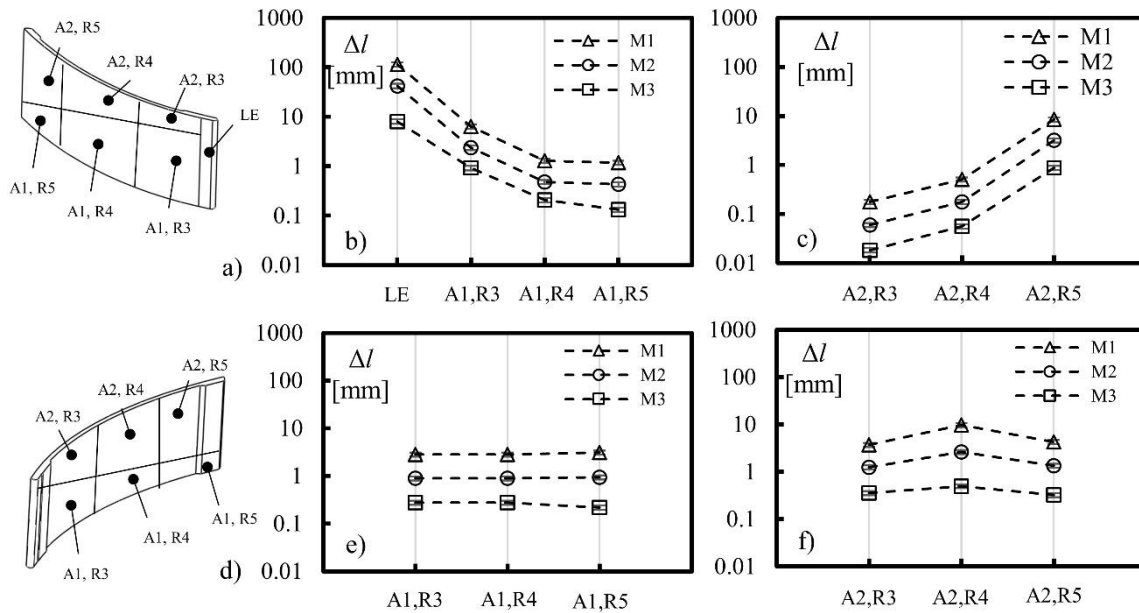


Figure 6: Rotor wear: a) coordinates of the patches on the pressure side, and material loss b) on the axial section A1 ; c) on the axial section A2; d) coordinates of the patches on the suction side, and material loss e) on the axial section A1 and f) on the axial section A2.

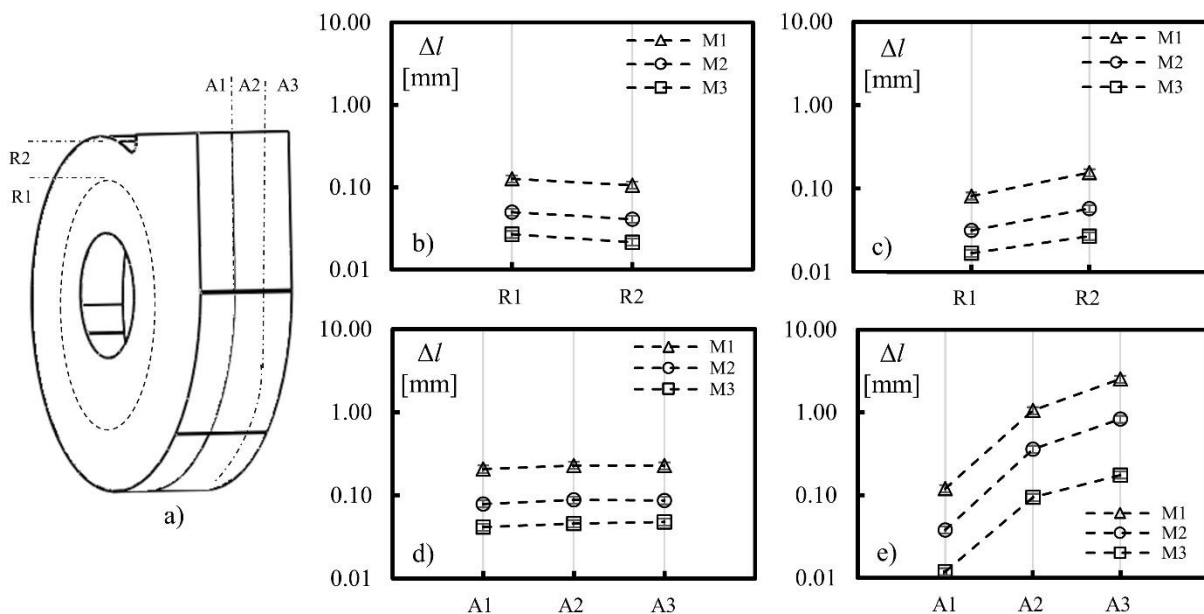


Figure 7: Volute wear: a) coordinates of the patches on volute, and material loss b) on the front side, c) backside, d) lateral side, and e) cut-off.

### Optimized configuration

The combination of numerical and experimental methods allowed to reliably assess the wear behavior of the fan operating with dust-laden flows. The results of the present work have been reported in terms of thickness reduction over 8,000 hours of operation: the usability of such



information has a key role in the estimation of the maintenance operation intervals along with the operative life of the machine. Customer warranty is, in fact, a serious concern for heavy-duty fan manufacturers, and its proper assessment could represent a huge competitive advantage in the field of heavy-duty machine supply. Another key role is played by the reduction of the costs without affecting the reliability and durability of the machine. It is obvious that the coverage of all the machine parts with the plate material with the highest wear resistance, without considering its price, will certainly ensure the highest possible durability. However, this strategy will automatically push the machine out of the market. Intending to reach a compromise between costs and durability, the results presented previously have been analyzed to identify an optimal configuration of the plate positioning. A thickness reduction of 3 mm over 8,000 hours of operation is set as an acceptable limit for the wear on the fan parts. This limit value has been chosen by considering that the hard-facing material of the plates has a thickness of 5 mm. According to this choice, after 8,000 hours of operation, inspections should be carried out to assess the overall condition of the machine.

The optimized configuration for the impeller is presented in Fig. 8 for the shroud (Fig. 6b), the hub (Fig. 6c), the pressure side (Fig. 6d), and the suction side (Fig. 6e). The plate materials have been positioned by combining their costs, their wear resistance, and the wear severity in the specific zone of the impeller. It can be noted that the material with the highest wear resistance (M3) is positioned only in the zones where the erosion severity does not allow the use of the cheapest materials (M1 and M2). Such zones are the leading edge (LE), a portion of the pressure side near the trailing edge (A2, R5), and a portion of the shroud in correspondence with the trailing edge (TE). Similarly, M2 is employed in the center of the disc (R1), in the first radial sector of the shroud (R3), in the first radial sector of the pressure side (A1, R3). The remaining parts of the impeller have been covered with M1. Looking at the stationary part, the low wear severity on the volute leads to the logical choice of using the material M1 for the front side, backside, and lateral side coverage. However, the high wear on the cut-off requires the positioning of M2 material only in this zone.

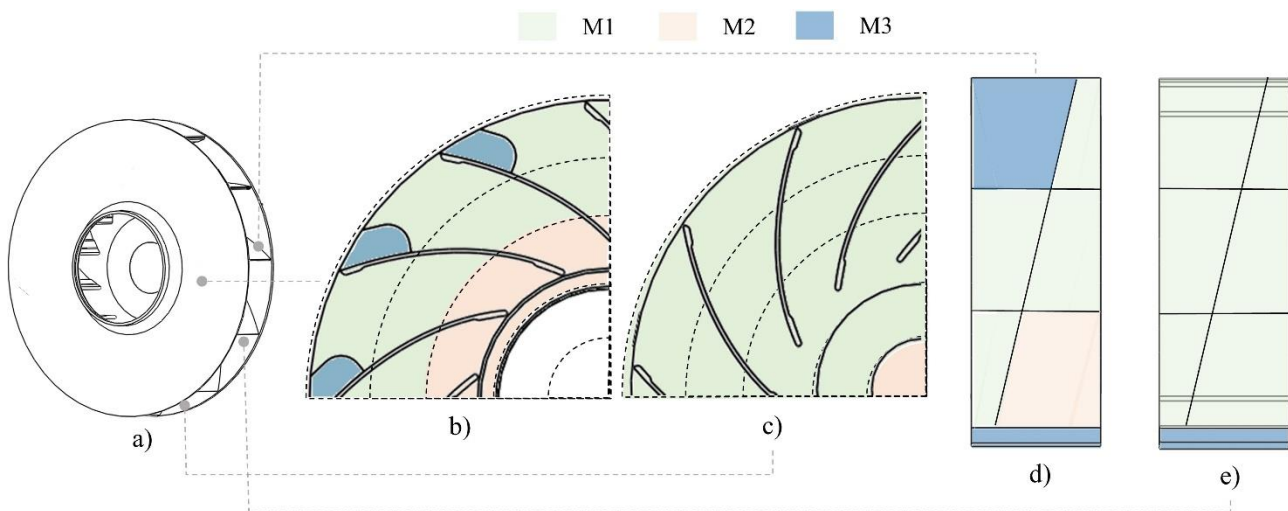


Figure 8: Optimized configuration of the wear-resistant plates on the rotor: a) view of the rotor, b) shroud, c) hub, d) pressure side, and e) suction side.

Even though such a solution can theoretically minimize the costs related to particle wear without compromising fan durability, it has to be highlighted that its implementation can be unpractical due to compatibility issues that may arise when different hard-facing plates are welded together. However, the approach reported in the present work can be adapted to practical applications for the only coverage of the zones most affected by particle wear.

## CONCLUSIONS

The present work is devoted to the assessment of the wear severity on the internal parts of a heavy-duty centrifugal fan and the optimization of the positioning of the wear-resistant plates along the flow path of the machine.

First, experimental tests have been carried out to assess the wear resistance of the hard-facing plates against the dust processed by the fan. A literature erosion model has been used to interpolate the experimental results to obtain mathematical relations capable of predicting the wear magnitude under general impact conditions. Then, a multiphase fluid dynamic simulation of the fan is carried out to assess the particle impacts on the rotating and stationary parts. The implementation of the erosion model, fed with experimental coefficients, led to the estimation of the wear severity on each fan zone.

The rotating parts are affected by a higher level of wear than stationary parts, and the leading edge is the zone affected by the highest material loss. The three hard-facing alloys show significant differences in terms of erosion resistance, due to their different properties and chemical composition. The results of the numerical analysis allowed implementing an optimized strategy for the wear-resistant plate positioning, pursuing cost reduction and increased fan durability.

## BIBLIOGRAPHY

- [1] Glasser, A. D., Petlevich, W. J., Sverdrup, E. F. – *Nature and costs of fan erosion in coal-fired electric power plants* (No. EPRI-CS-1596). Westinghouse Electric Corp., Pittsburgh, PA (USA). Research Labs, **1980**
- [2] Cardillo, L., Corsini, A., Delibra, G., Rispoli, F., Sheard, A. G., Venturini, P. – *Simulation of particle-laden flows in a large centrifugal fan for erosion prediction*. In Turbo Expo: Power for Land, Sea, and Air (Vol. 45578, p. V01AT10A014). American Society of Mechanical Engineers, **2014**
- [3] Castorrini, A., Venturini, P., Corsini, A., Rispoli, F. – *Numerical simulation of the blade aging process in an induced draft fan due to long time exposition to fly ash particles*. Journal of Engineering for Gas Turbines and Power, 141(1), 011025, **2019**
- [4] Aldi, N., Casari, N., Pinelli, M., Suman, A., Vulpio, A., Saccenti, P. – *Performance Modification of an Erosion-Damaged Large-Sized Centrifugal Fan*. In Turbo Expo: Power for Land, Sea, and Air (Vol. 84898, p. V001T10A011). American Society of Mechanical Engineers, **2021**
- [5] Finnie, I., and McFadden, D. H. – *On the velocity dependence of the erosion of ductile metals by solid particles at low angles of incidence*. Wear 48.1, 181-190, **1978**
- [6] ASTM G76-04. - *Standard test method for conducting erosion tests by solid particle impingement using gas jets*, **2004**
- [7] Schrade, M., Staudacher, S., Voigt, M. – *Experimental and numerical investigation of erosive change of shape for high-pressure compressors*. In Turbo Expo: Power for Land, Sea, and Air (Vol. 56628, p. V001T01A001). American Society of Mechanical Engineers, **2015**
- [8] Oka, Y. I., Okamura, K., Yoshida, T. – *Practical estimation of erosion damage caused by solid particle impact: Part 1: Effects of impact parameters on a predictive equation*. Wear, 259(1-6), 95-101, **2005**
- [9] Aldi, N., Casari, N., Pinelli, M., Suman, A., Vulpio, A., Saccenti, P., Beretta, R., Fortini, A., Merlin, M. – *Erosion behavior on a large-sized centrifugal fan*. In Proceedings of the 13th European Turbomachinery Conference on Turbomachinery Fluid Dynamics and Thermodynamics, ETC (pp. 1-8), **2019**